Reflow Recipe Establishment Based on CFD-Informed Machine Learning Model

Yangyang Lai, *Graduate Student Member, IEEE*, Jong Hwan Ha, Karthik Arun Deo, Junbo Yang, Pengcheng Yin, *Graduate Student Member, IEEE*, and Seungbae Park, *Senior Member, IEEE*

***Abstract*— This article proposes a computational fluid dynamics (CFD)-based machine learning (ML) model to set the temperature of a convection reflow oven and control conveyor speed. Due to the thermal mass variation of printed circuit boards (PCBs) and surface mount components, the reflow recipe should be specified for each PCB assembly individually. Instead of relying on process engineers' skills and experience, the ML model supported by heat transfer mechanisms provides a clear and logical path in the reflow recipe setup. An ideal recipe should let the largest component reach the minimum reflow temperature; meanwhile, the temperature cannot damage the small or heat-sensitive components. To simulate the reflow soldering process, the CFD model was used after being validated with experiment results. A system was programmed to feed the output of the CFD model as the input to the ML model. Benefiting from the interpolation and fast response brought by ML models, we can rapidly obtain the results subjected to millions of recipes, which are the combination of preset temperatures of all the heating zones and the conveyor speed in the oven. Using a weighting filter function, the optimal recipe can be obtained. This methodology is especially beneficial to reflowing smaller batches of complex PCB assemblies with a big heat capacity.**

***Index Terms*— Computational fluid dynamics (CFD), reflow soldering, regression model, surface-mount technology (SMT).**

I. INTRODUCTION

REFLOW soldering is the process to assemble electronic components onto printed circuit boards (PCBs) by reflowing solder paste to form robust joints. Reflow profiling is to measure the temperatures of several points on the board to determine whether the process is in control or not [1]. Insufficient heating and overheating can result in solder defects (e.g., skewing, bridging, voiding, and insufficient wetting) and device reliability issues [2], [3]. Because of the thermal mass variation of PCB and surface-mount components, the reflow recipe should be specified for each PCB assembly individually. An ideal recipe should let the largest component reach the minimum reflow temperature; meanwhile, the temperature cannot damage the small or heat-sensitive components [1], [4].

Manuscript received 26 September 2022; revised 5 January 2023; accepted 19 January 2023. Date of publication 23 January 2023; date of current version 15 February 2023. Recommended for publication by Associate Editor X. Fan upon evaluation of reviewers' comments. *(Corresponding author: Yangyang Lai.)*

The authors are with the Department of Mechanical Engineering, State University of New York at Binghamton, Binghamton, NY 13850 USA (e-mail: ylai9@binghamton.edu).

Color versions of one or more figures in this article are available at https://doi.org/10.1109/TCPMT.2023.3239304.

Digital Object Identifier 10.1109/TCPMT.2023.3239304

If the cold spot and hot spot are controlled, the temperatures across the board can be within a safe range, which is the reflow profile band.

Though vapor phase soldering is an ideal technology for assemblies with a large variety of thermal mass, its high running cost and low throughput make the convection oven always the first choice in large-scale production [5], [6], [7]. For decades, reflow profiling is based on process engineers' skills and experience. The objective of this work is to provide a clear and logical approach to establishing reflow recipes, especially for the board assembly with thick PCB and bulky components. Compared with tedious trial and error, this approach significantly decreases labor costs and time consumption. By changing the criteria of the data rater, the model can provide several reflow recipes at varied conveyor speeds, which is quite helpful when balancing the throughput and thermomechanical reliability of the bulky component.

Numerical methods, such as computational fluid dynamics (CFD) models, are widely used to optimize the reflow soldering [8], [9]. Shao et al. [10] employed the CFD model to obtain the temperature distribution of the 2.5-D package and mapped it to a thermomechanical model to predict package deformation. Lai et al. [11], [12] used the CFD model to compare the temperatures of solder joints of packages with different thermal masses in the reflow process. Deng et al. [13] predicted the temperature of a system in package assembly using CFD modelsClick or tap here to enter text. Lau and Abdullah [14] conducted the thermal analysis for PCB assembly using CFD models to obtain temperatures of solder balls during the reflow process.

In this work, the solder joint temperatures of the component with the greatest thermal mass were simulated using the CFD model. The solder ball at the center of a ball grid array (BGA) is regarded as the cold spot across the board. The surface temperature of PCB is the hot spot, which is followed by the temperatures of small-size components. The CFD model was validated using the results of measurements. To ensure that the reflow profiles of both extreme spots were within the safe band, trial and error is required to find the appropriate boundary conditions, which are the temperatures of all the heating zones and the conveyor speed. The number of zones in the reflow oven determines the complexity of the combination of boundary conditions. To ease the computation cost, the machine learning (ML) model informed by the CFD model is employed to predict the reflow profiles.

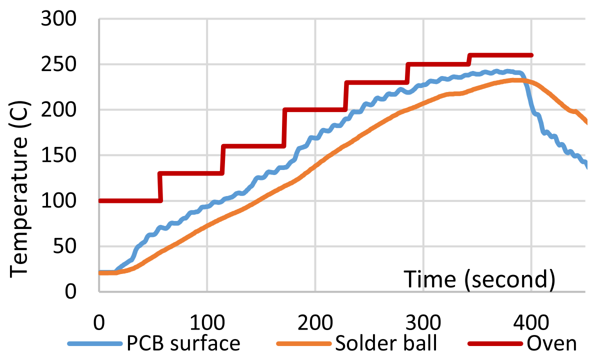

Fig. 1. Reflow profiles of extreme limits.

Machine learning models have been widely used in surface-mount technology (SMT) assembly, such as solder paste printing, component placement, and reflow soldering. Zhancheng et al. [15] used a support vector machine (SVM) model to predict the real process temperatures at several points of the PCBClick or tap here to enter text. Tsai [16] proposed a neuro-computing approach to study the second side reflow profiles of PCB assemblies. Lam [17] proposed a noncontact approach to predict the temperature distribution of PCB during the reflow process. Li et al. [18] developed an artificial neural network to predict the reflow profile of the PCB surface, which achieved the 97.2% accuracy.

The ML model used in this study is trained by the data exported from the CFD model. By replacing repetitive parts of the CFD model with an efficient ML model, the boundary conditions corresponding to the ideal reflow profile can be rapidly obtained in reverse. The heat transform problem is transformed into several regression models. The model inputs are preset temperatures of the reflow oven, conveyor speed, and physical information of the critical component. The outputs are peak temperatures and time above liquidus (TAL), which are used for reflow profile evaluation. Because of the rapid response of ML models, millions of results corresponding to the varied reflow recipes can be gotten in seconds. By filtering and sorting as per the industrial standard, the optimal reflow recipe can be obtained. This approach is not intended to replace the experiment using the profiling board but to decrease the cost of trial and error.

II. Interpretation of Reflow Profile

When a large thermal mass differential exists on a board, it is difficult to maintain a uniform temperature distribution across the board. The objective of reflow profiling is to keep all profiles within the safe band by limiting extreme conditions. As shown in Fig. 1, PCB surface temperature, which is the upper limit profile, is determined by the heat capacity of the PCB. The temperature of the solder ball between the PCB and the BGA component, which is the lower limit profile, is determined not only by PCB but also by the component with the greatest thermal mass.

As shown in Fig. 2, the temperature profiles of five PCBs with varied thicknesses were collected. The peak temperatures of the five PCBs subjected to the identical reflow recipe vary from 207 °C to 240 °C. Though the specific heat of PCBs is unknown, their thicknesses can reflect their thermal mass. The board's temperature is affected significantly by its thermal mass.

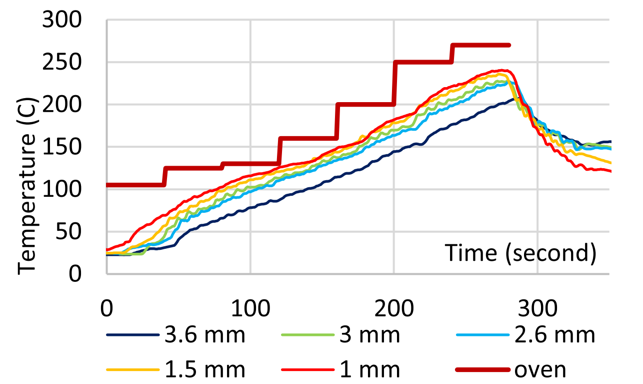

Fig. 2. Reflow profiles of PCB with varied thicknesses.

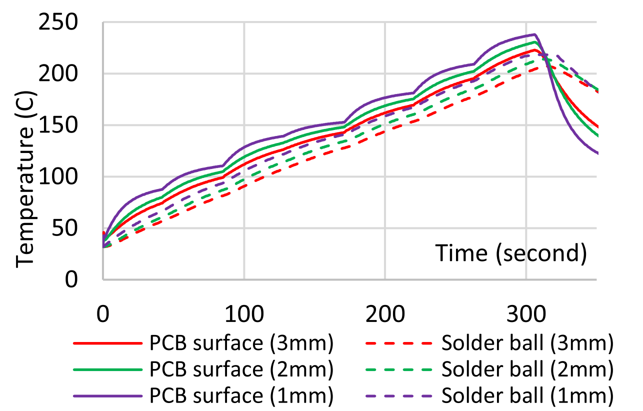

Fig. 3. Reflow profiles of identical components on PCB with varied thicknesses.

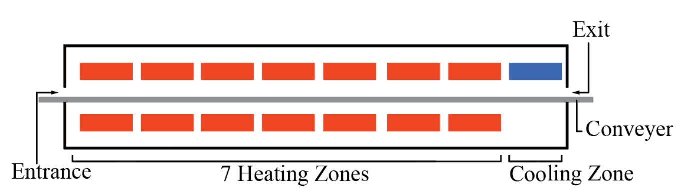

Fig. 4. Schematic of the reflow oven.

As shown in Fig. 3, the reflow profiles of a component (solder ball) on PCBs with varied thicknesses were simulated using the CFD model, which is introduced in Section III. The gaps between PCB surface temperature and solder ball temperature are almost identical. The peak temperature differences of a PCB surface and solder ball are all in the range of 16 °C–19 °C. This observation verifies the opinion that once the upper limit is fixed, the gap between upper and lower limit profiles is determined by the component with the biggest thermal mass.

III. CFD Model Development and Validation

A. Field Measurement

As shown in Fig. 4, a seven-zone reflow oven is used in this work. The temperature in each zone can be independently

TABLE I
TEMPERATURE SETTING

Zone	1	2	3	4	5	6	7
T (°C)	105	125	150	175	220	270	280

TABLE II
CONVEYOR SPEED

Conveyor speed (cm/min)	45	35	25
Heating time (second)	271	341	471

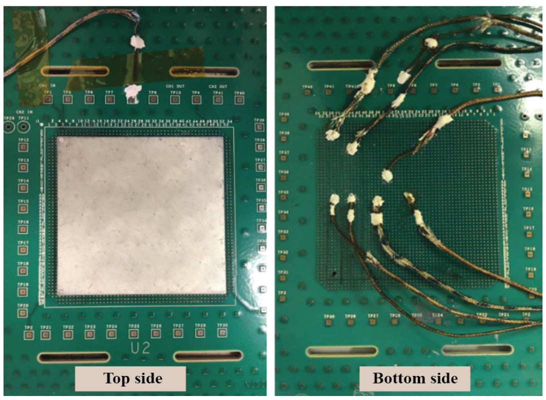

Fig. 5. PCB with flip-chip lidded BGA package.

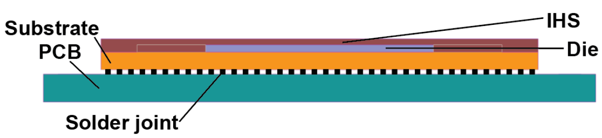

Fig. 6. Schematic of the BGA package.

TABLE III
DIMENSIONS OF THE BGA PACKAGE

Material	Dimensions (mm)
PCB	140 x 90 x 3.1
Integrated Heat Spreader (IHS)	47.5 x 47.5 x 1.43
Solder joint	Height: 0.45, Pitch: 1.0
Die	35 x 25 x 0.8
Substrate	47.5 x 47.5 x 1.9

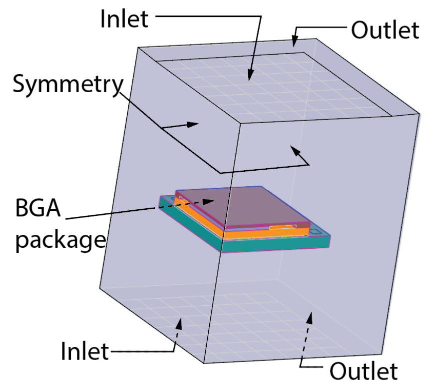

Fig. 7. Schematic of the CFD model.

TABLE IV
MATERIAL PROPERTIES OF AIR

Property	Polynomial equations of temperature, T (K)
K (W/m.K)	K = 6.79E-05T+ 5.51E-03
Cp (J/kg.K)	Cp = 4.00E-04T2 - 2.06E-01T + 1.03E+03
ρ (kg/m3)	ρ = 4.99E-06T2 - 6.33E-03T + 2.61E+00

controlled with the closed-loop control system [19]. The PCB assembly is transported through each heating zone and cooled in the cooling zone before exiting the oven. The temperature of each zone was preset according to Table I. The ramp rate (room temperature to peak temperature) is associated with conveyor speed. Considering the boundary independence for the CFD model validation, measurements were conducted at three conveyor speeds, as shown in Table II.

The PCB assembly used is shown in Fig. 5. K-type thermocouples were embedded on the top side of the PCB to monitor the board surface temperature. Other thermocouples were attached to the pads through drilled holes to monitor the temperatures of solder joints. Solder material absorbs and releases latent heat during the reflow process and influences the shape of the reflow profile at the melting point. Thus, the plateau on the profile at around 217 °C can prove that the solder temperature is captured successfully. MEGA M.O.L.E. thermal profiler was used to collect transient data during the reflow process. The accuracy of the profiler is ±1 °C.

B. CFD Model

The structure of the BGA package is shown in Fig. 6. The dimension of every part inside the package is listed in Table III. Small features, such as leads, thermal interface material, via, and underfill, are not included in this compact model because computing such a detailed model is not practical in a board-level simulation [20], [21], [22], [23], [24].

As shown in Fig. 7, the quarter symmetric geometry was molded in ANSYS-FLUENT. To achieve more efficient performance, polyhedral meshing was selected instead of other meshing methods, such as tetrahedral or hybrid meshes. The transient solver was used with K-epsilon turbulence and SIMPLE pressure–velocity coupling mode. Meshing size independence of the CFD model was considered for the solid and fluid portions. Finer mesh granules were used until stable results were achieved. Meanwhile, the transient residual error was kept 10^{-3} below as the convergence criterion. To compare the model stability with varied element amounts, the peak temperature of the solder joints was used in the comparison. The element amount was finalized to 136 011. This is only for the model used in validation; the element amount will change to some extent after changing the package geometry for the later work.

The thermal properties of air were set in polynomial equations of temperature, as shown in Table IV [25], [26]. SAC305 solder joints are the interconnection between the

TABLE V

MATERIAL PROPERTIES OF THE BGA PACKAGE

Material	K (W/m.K)	Cp (J/kg.K)	D (kg/m3)
Silicon	98.4	721	2300
PCB	0.5	1405	2252
Solder	58	232	7380
Substrate	0.2	920	1700
Copper	392	387	8940

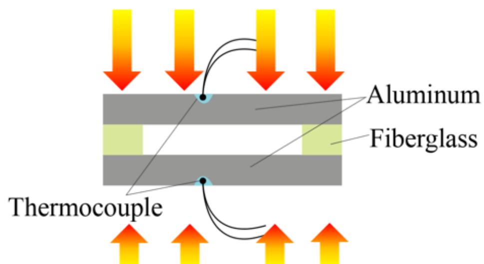

Fig. 8. Aluminum boards with thermocouples.

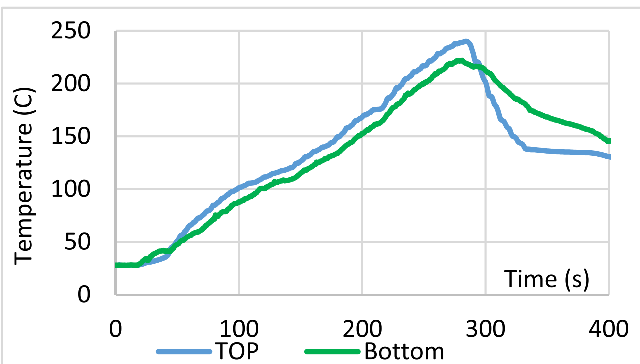

Fig. 9. Measurement results of upper and lower inlets.

component and PCB. Because the solder paste experiences phase transformations, the latent heat is considered in the simulation. The pure solvent melting heat of SAC 305 is 53.08 J/g [27]. Solidus and liquidus temperatures of the solder are 217 °C and 220 °C, respectively. The material properties of other materials are listed in Table V [28], [29].

Because of the different airflow at upper and lower inlets, their boundary conditions should be set individually. Two pieces of aluminum boards with thermocouples were used to collect the measurement data, as shown in Fig. 8. Because of the better thermal conductivity, the aluminum boards can collect data with more accuracy and less deviation compared with the organic board. To make sure that each aluminum board receives energy unidirectionally, fiberglass was used to insulate them from each other. As shown in Fig. 9, the energy delivered from the top is much more than from the bottom because of the specification difference between the blowers and oven structures on the two sides.

C. Model Validation

The temperatures of the PCB surface and solder joint at the center of the BGA were used to tune the CFD model.

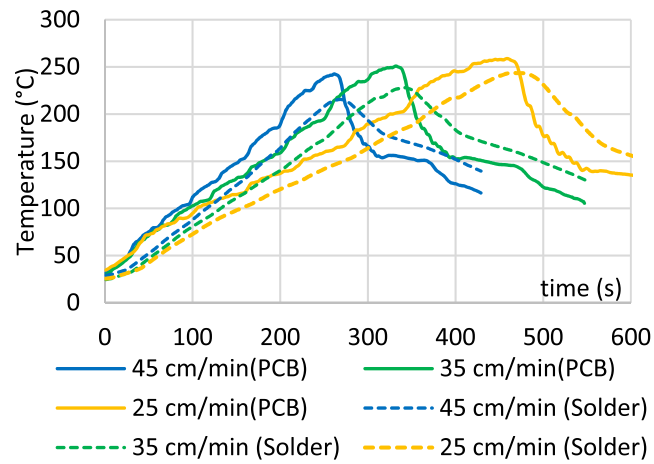

Fig. 10. Reflow profiles at three conveyor speeds.

TABLE VI

SIMULATION RESULTS VERSUS MEASUREMENT RESULTS

Parameter	Difference	Error
Board peak temperature	2.35 °C	1%
Board Time above liquidus	1.1 second	0.71%
Solder_Peak temperature	1.606 °C	0.67%
Solder_Time above liquidus	0.5 second	0.60%

TABLE VII

INPUT FACTORS

Package dimensions		
PCB thickness	Substrate thickness	Die thickness
3 mm	1.9 mm	0.8 mm
2 mm	0.9 mm	0.4 mm
1 mm		

Reflow recipe				
Zone 4	**Zone 5**	**Zone 6**	**Zone 7**	**conveyor speed**
180 °C	220 °C	260 °C	280 °C	25 cm/min
210 °C	250 °C	270 °C	290 °C	35 cm/min
240 °C	270 °C	280 °C	300 °C	45 cm/min

Considering the boundary condition independence, the CFD model was correlated with three sets of measurement results, as shown in Fig. 10. The peak temperature and TAL of measurement results were used to compare with the simulation results, as shown in Table VI. The error of four parameters shows that the CFD model is compatible with the measurement results. The errors are within 1%. Hence, the CFD model can simulate the reflow process.

IV. MACHINE LEARNING MODEL

A. Python-Fluent Coupling System

To automatically generate the training data for the ML model, a system was programmed to couple the ANSYS-FLUENT with a Python session.

To relieve the training data demand, the preset temperatures of zones 1–3 were not selected as input factors and fixed at 105 °C, 125 °C, and 145 °C, respectively. The more toward

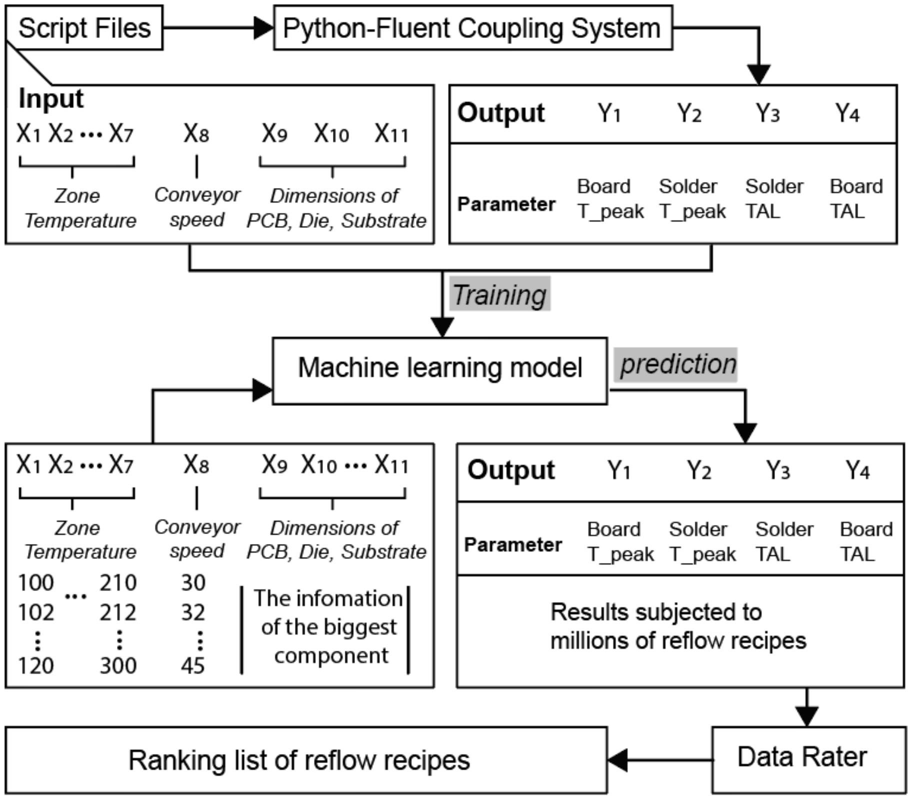

Fig. 11. Flowchart of model training and prediction.

the front the zone is, the less influence it has on the reflow profile. In this study, the temperatures of zones 4–7 and conveyor speed were set as the input factors. There are three candidate values for each input factor, as shown in Table VII. Package assemblies have three dimensions, of course, but we considered only the thickness because the dominant heat transfer during reflow occurs vertically. From the equation of heat transfer rate

$$Q = UA\Delta T \tag{1}$$

where Q is the heat transfer (W), U is the overall heat transfer coefficient (W/m^{2}K), A is the wall area (m^2), and ΔT is the temperature difference over wall (°C).

Equation (1), which governs the heat transfer rate, shows that width and length are important, but we ignored them to limit the amount of needed training data. For each model geometry, the scripts with 243 sets of boundary conditions were generated and imported into fluent sequentially.

The flowchart of the model training and prediction process is shown in Fig. 11. The peak temperature and TAL of the PCB surface and solder joint were extracted from the simulated results as the output factors. The peak temperature and TAL on the board surface, which occurs at the hot spot, are controlled to prevent overheating small and heat-sensitive components. The peak temperature and TAL of the solder joint are used to make sure that the cold spot reaches the minimum temperature that allows a successful reflow of all the solder balls.

TABLE VIII
IMPACT INDEX

Impact index	Parameter	Effect
I_1	Board peak temperature	Risk for small components
I_2	Board TAL	
I_3	Conveyor speed	Efficiency

B. ML Model Training

A Gaussian process regression model is used in this application. With fivefold cross validation, the root-mean-square error (RMSE) of Y_1 and Y_2 is below 0.38, and the RMSE of Y_3 and Y_4 reach an error below 1.6. Because the training data are from a simulation without interference noise, a good performance is not surprising.

In the prediction process, once the dimensions of the biggest component and PCB are given to ML models, the outputs subjected to millions of recipes can be obtained in seconds.

C. Optimal Recipe

A data rater was programmed to eliminate, sort, and rank the output results and export the best three sets of reflow recipes. Unqualified data are eliminated based on two criteria. The peak temperature of the central solder (Y_1) should reach 230 °C, and its TAL (Y_4) should reach 60 s [30]. This step ensures that the minimum reflow temperature is reached in the cold spot, which is at the center of the biggest component. The threshold values of Y_1 and Y_4 are from solder paste companies, component

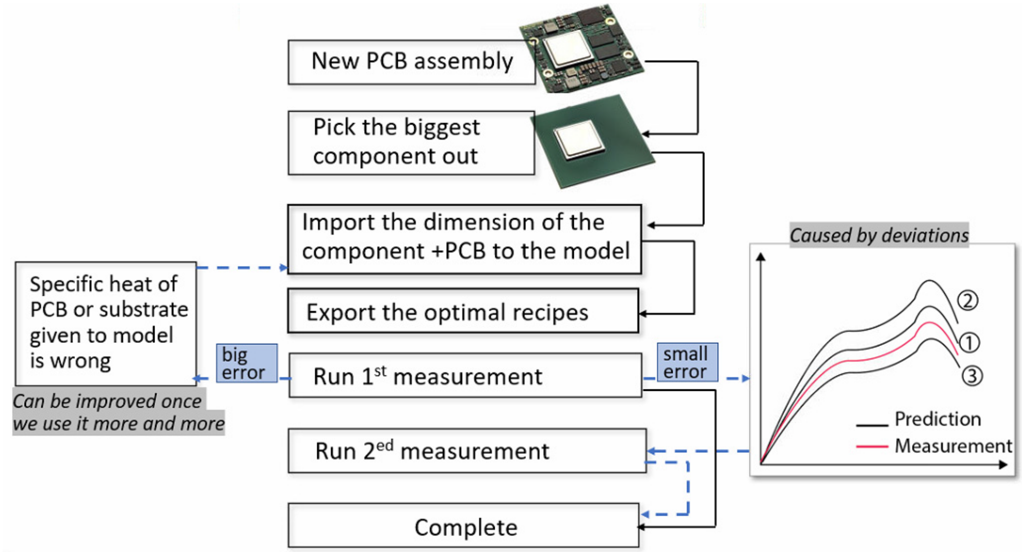

Fig. 12. Flowchart of model application.

TABLE IX
RESULTS OF INITIAL SETUP AND ADJUSTMENT

Recipe	Zone 4 (°C)	Zone 5 (°C)	Zone 6 (°C)	Zone 7 (°C)	Conveyor speed (cm/min)	Peak temperature (°C)		TAL (second)		
						Board	Solder	Solder	Board	
One	217	226	250	260	32	243	230	78	49	Prediction
						240	225	86	44	Measurement
						3 (1.3%)	5 (2.2%)	8 (9.3%)	5(11.4%)	Error
Two	217	244	258	260	32	246	235	100	69	Prediction
						242	231	101	73	Measurement
						4 (1.7%)	4 (1.7%)	1 (1.0%)	4(5.5%)	Error
Three	220	250	254	258	30	246	237	111	79	Prediction
						244	233	130	92	Measurement
						2 (1.0%)	4 (1.7%)	15 (1.3%)	14(1.3%)	Error

suppliers, and the JEDEC standard. After that, the remaining data are sorted by the peak temperature and TAL of the board (Y_2 and Y_3) in ascending order. P_1 and P_2 are the orders of the sorted data. This step controls the board surface temperature, which is related to the small, heat-sensitive components. P_3, the order of data sorted by the conveyor speed, is used to denote the throughput. The weight function method is used to rate each set of recipes. Impact indexes I_1–I_3 denote the weight of each parameter (P_{1-3}), as shown in Table VIII. The optimal recipes were ranked by the score calculated by the following weight function:

$$\text{Score} = I_1 \times P_1 + I_2 \times P_2 + I_3 \times P_3. \tag{2}$$

Because of the deviation among ML models, CFD model, and experiment, it is recommended to output three sets of recipes by changing the criteria for Y_1 and Y_4. Once the difference between measurement and prediction is met, the two backup options can be used for fine-tuning.

It is needed to emphasize that there is no perfect profile. The solder paste specifications allow quite a large process window, which are the two criteria used in data elimination. After meeting the basic criteria, the optimal recipe can be customized using the three impact index. The conveyor speed (I_3) can be given more weight if throughput is prioritized over the others. If the component supplier gives a strict requirement regarding temperature, then I_1 should be given more weight.

V. Application Using the ML Model

A. Flowchart of the Model Application

The flowchart in Fig. 12 shows how to apply the ML model to new PCB assemblies. Once a new PCB assembly is given, pick out the component with the biggest thermal mass. After inputting the dimensions of the biggest component and PCB into the model, the results subjected from millions of recipes are output rapidly. Based on the criteria given, the model can output three sets of optimal recipes for the initial oven setup. If the measurement based on recipe #1 is acceptable, the job is completed. If the difference between the first run measurement and the prediction is a small error, which is caused by the deviations between the ML model, CFD model, and experiment, it is recommended to try recipe #2 or #3 as the fine-tuning process. In some cases, the error is out of the reasonable range. The biggest errors are always caused by the incorrect material properties of composite materials such as substrate or PCB. Based on the first run measurement, the thermal mass of PCB or substrate should be adjusted, and the model will regenerate new optimal recipes. This problem can be improved once we use the ML model more.

B. Results of the Model Validation

The results of the prediction and measurement of the PCB assembly based on the ML model are shown in Table IX. First, the oven was set as per recipe #1. The measured peak temperature of the solder joint did not reach 230 °C, which is the bottom line of solder joints. Therefore, recipe #2 was selected for the fine-tuning process. Then, all the parameters, including peak temperature and TAL of solder joints and board surface, are within the acceptable range. The ramp rate is 0.63 °C/s, which is higher than the bottom line, 0.5 °C/s. The hottest temperature that the oven reached was 260 °C, which is a very safe setting.

The error of peak temperature is below 2.5%. The TAL error reaches 15% because the thermocouples used to measure the solder temperature were embedded below the copper pad, not directly in contact with the solder joints. Also, the solder temperature stays around the melting point for a long time because of the latent heat effect. Thus, small temperature tolerance can generate a bigger error concerning time. However, the TAL error is still acceptable because of the large process window of TAL, 30–120 s.

VI. Conclusion

This article proposes a novel approach to establishing reflow recipes, especially for the board assembly with thick PCB and bulky components. The CFD model used to simulate the reflow process was validated using field measurement data. A system was programmed to generate 2916 sets of simulation results with varied boundary conditions and model geometries. The outputs of the CFD model were continually fed to the ML model as the training data. A Gaussian process regression model was used for prediction and its RMSE was below 1.6.

Benefiting from the interpolation and fast response brought by ML models, the optimal recipe was obtained within two measurements, which took less than half an hour. Compared with tedious trial and error, this approach significantly decreases labor costs and time consumption. By changing the criteria of the data rater, the ML model can provide several sets of reflow recipes at varied conveyor speeds, which is quite helpful when balancing the throughput and thermomechanical reliability of the bulky component. This approach is not intended to replace the experiment using the profiling board but to decrease the cost of trial and error.

In this study, we only focus on the lidded BGA package, which is the most typical packaging type for bulky components. This model cannot serve the other types of packages, such as bare die packages and molded packages. Additional models are needed for other types of packages individually, which is the constraint of this approach. In the meanwhile, there has been a rise in the popularity of breaking down large monolithic die into chiplets in a single module, so the package's internal structures vary from each other. A more universal model will be developed to address the heterogeneously integrated packages. How to balance the compactness, universality, and accuracy of the model is the future work of this study.

References

[1] R. Lasky and E. Briggs, "Best practices reflow profiling for lead-free SMT Assembly," Indium Corp., Dartmouth College, Clinton, NY, USA, Tech. Rep. 98675, 2009.

[2] Y. Lai et al., "An intelligent system for reflow oven temperature settings based on hybrid physics-machine learning model," *Soldering Surf. Mount Technol.*, vol. 34, no. 5, pp. 266–276, Sep. 2022, doi: 10.1108/ssmt-10-2021-0063.

[3] K. Arun Deo, R.-N. Kono, C. Cai, J. Yang, Y. Lai, and S. Park, "A study on parameters that impact the thermal fatigue life of BGA solder joints," in *Proc. ASME Int. Tech. Conf. Exhib. Packag. Integr. Electron. Photon. Microsyst.*, Oct. 2022, pp. 1–9, doi: 10.1115/IPACK2022-97253.

[4] J. Ha et al., "Shape dependency of fatigue life in solder joints of chip resistors," in *Proc. IEEE 72nd Electron. Compon. Technol. Conf. (ECTC)*, May 2022, pp. 1489–1494, doi: 10.1109/ECTC51906.2022.00237.

[5] A. Géczy, B. Kvanduk, B. Illes, and G. Harsányi, "Comparative study on proper thermocouple attachment for vapour phase soldering profiling," *Soldering Surf. Mount Technol.*, vol. 28, no. 1, pp. 7–12, Feb. 2016, doi: 10.1108/SSMT-10-2015-0033.

[6] I. Bozsóki, B. Illés, and A. Géczy, "Compact numerical modelling of transient condensate layer formation on small components during vapour phase soldering," *Int. Commun. Heat Mass Transf.*, vol. 135, Jun. 2022, Art. no. 106071, doi: 10.1016/j.icheatmasstransfer.2022.106071.

[7] D. Straubinger, B. Illés, D. Busek, N. Codreanu, and A. Géczy, "Modelling of thermocouple geometry variations for improved heat transfer monitoring in smart electronic manufacturing environment," *Case Stud. Thermal Eng.*, vol. 33, May 2022, Art. no. 102001, doi: 10.1016/j.csite.2022.102001.

[8] Y. Lai et al., "A deep learning approach for reflow profile prediction," in *Proc. IEEE 72nd Electron. Compon. Technol. Conf. (ECTC)*, May 2022, pp. 2269–2274, doi: 10.1109/ECTC51906.2022.00358.

[9] Y. Lai et al., "The optimal solution of reflow oven recipe based on physics-guided machine learning model," in *Proc. 21st IEEE Intersoc. Conf. Thermal Thermomech. Phenomena Electron. Syst. (iTherm)*, May 2022, pp. 1–6.

[10] S. Shao et al., "Comprehensive study on 2.5D package design for board-level reliability in thermal cycling and power cycling," in *Proc. IEEE 68th Electron. Compon. Technol. Conf. (ECTC)*, May 2018, pp. 1668–1675, doi: 10.1109/ECTC.2018.00251.

[11] Y. Lai, K. Pan, J. Xu, J. Yang, and S. Park, "Determination of smarter reflow profile to achieve a uniform temperature throughout a board," in *Proc. 20th IEEE Intersoc. Conf. Thermal Thermomech. Phenomena Electron. Syst. (iTherm)*, Jun. 2021, pp. 911–916.

[12] Y. Lai, K. Pan, C. Cai, P. Yin, J. Yang, and S. Park, "Smarter temperature setup for reflow oven to minimize temperature variation among components," *IEEE Trans. Compon., Packag., Manuf. Technol.*, vol. 12, no. 3, pp. 562–569, Mar. 2022, doi: 10.1109/TCPMT.2022.3153952.

[13] S.-S. Deng, S.-J. Hwang, and H.-H. Lee, "Temperature prediction for system in package assembly during the reflow soldering process," *Int. J. Heat Mass Transf.*, vol. 98, pp. 1–9, Jul. 2016, doi: 10.1016/j.ijheatmasstransfer.2016.03.008.

[14] C.-S. Lau and M. Z. Abdullah, "Simulation investigations on fluid/structure interaction in the reflow soldering process of board-level BGA packaging," *Int. J. Comput. Theory Eng.*, vol. 5, no. 4, pp. 645–649, 2013, doi: 10.7763/ijcte.2013.v5.767.

[15] Z. Wang, W. Li, H. Tong, and Y. Xu, "A novel on-board temperature monitoring approach in the reflow soldering process," in *Proc. IEEE/RSJ Int. Conf. Intell. Robots Syst.*, Oct. 2006, pp. 4245–4251, doi: 10.1109/IROS.2006.281952.

[16] T. Tsai, "Development of an integrated reflow soldering control system using incremental hybrid process knowledge," *Expert Syst. Appl.*, vol. 28, no. 4, pp. 681–692, May 2005, doi: 10.1016/j.eswa.2004.12.025.

[17] T. L. Lam, "Low-cost non-contact PCBs temperature monitoring and control in a hot air reflow process based on multiple thermocouples data fusion," *IEEE Access*, vol. 4, pp. 123566–123574, 2020, doi: 10.1109/ACCESS.2020.3036527.

[18] Y. Li, J. He, D. Won, and S. W. Yoon, "Noncontact reflow oven thermal profile prediction based on artificial neural network," *IEEE Trans. Compon., Packag., Manuf. Technol.*, vol. 11, no. 12, pp. 2229–2237, Dec. 2021, doi: 10.1109/TCPMT.2021.3120310.

[19] B. Illés and I. Bakó, "Numerical study of the gas flow velocity space in convection reflow oven," *Int. J. Heat Mass Transf.*, vol. 70, pp. 185–191, Mar. 2014, doi: 10.1016/j.ijheatmasstransfer.2013.10.075.

[20] J. Yang et al., "A comparison study of TIM degradation of phase change material and thermal grease," in *Proc. IEEE 71st Electron. Compon. Technol. Conf. (ECTC)*, Jun. 2021, pp. 1978–1983, doi: 10.1109/ECTC32696.2021.00312.

[21] K. Pan, C. Okoro, Y. Lai, D. Joshi, S. Park, and S. Pollard, "A comparative study of the thermomechanical reliability of fully-filled and conformal through-glass via," in *Proc. IEEE 72nd Electron. Compon. Technol. Conf. (ECTC)*, May 2022, pp. 1211–1217, doi: 10.1109/ECTC51906.2022.00194.

[22] K. Pan et al., "Investigation of copper and glass interaction in through glass via (TGV) during thermal cycling," in *Proc. IEEE 71st Electron. Compon. Technol. Conf. (ECTC)*, Jun. 2021, pp. 1660–1666, doi: 10.1109/ECTC32696.2021.00263.

[23] K. Pan et al., "In-situ temperature-dependent characterization of copper through glass via (TGV)," *Microelectron. Rel.*, vol. 129, Feb. 2022, Art. no. 114487, doi: 10.1016/j.microrel.2022.114487.

[24] Y. Lai et al., "Thermomechanical reliability of BGA packages with different underfill reinforcement methods," in *Proc. ASME Int. Tech. Conf. Exhib. Packag. Integr. Electron. Photon. Microsyst.*, Oct. 2022, pp. 1–6, doi: 10.1115/IPACK2022-97349.

[25] K. Dusek, C. Stancu, P. V. Notingher, P. Mach, and M. Placek, "Experimental and numerical analysis of melting and solidification of SnAgCu joints," *IEEE Trans. Compon., Packag., Manuf. Technol.*, vol. 6, no. 9, pp. 1445–1455, Sep. 2016, doi: 10.1109/TCPMT.2016.2593709.

[26] H. Yu, T. T. Mattila, and J. K. Kivilahti, "Thermal simulation of the solidification of lead-free solder interconnections," *IEEE Trans. Compon. Packag. Technol.*, vol. 29, no. 3, pp. 475–485, Sep. 2006, doi: 10.1109/TCAPT.2005.848590.

[27] C. Bailey, D. Wheeler, and M. Cross, "Numerical modelling of solder joint formation," *Soldering Surf. Mount Technol.*, vol. 10, no. 2, pp. 6–13, Aug. 1998, doi: 10.1108/09540919810219912.

[28] C.-S. Lau, M. Z. Abdullah, and F. C. Ani, "Computational fluid dynamic and thermal analysis for BGA assembly during forced convection reflow soldering process," *Soldering Surf. Mount Technol.*, vol. 24, no. 2, pp. 77–91, 2012, doi: 10.1108/09540911211214659.

[29] S. Liang, W. Mingxiang, H. YongHong, L. Tim Fai, and J. Y. Qi, "Reflow profile simulation by finite element method for a BGA package," in *Proc. 6th Int. Conf. Electron. Packag. Technol.*, 2005, pp. 6–9, doi: 10.1109/ICEPT.2005.1564717.

[30] *Joint Industry Standard Moisture/Reflow Sensitivity Classification for Nonhermetic Surface Mount Devices*, Solid State Technol. Assoc., Arlington, VA, USA, 2014.

Yangyang Lai (Graduate Student Member, IEEE) received the M.S. degree in mechanical engineering from the State University of New York at Binghamton, Binghamton, NY, USA, in 2021, where he is currently pursuing the Ph.D. degree.

His current research interests include the optimization of reflow soldering using hybrid numerical and machine learning approaches, and accessing the thermal reliability of electronic packages.

Jong Hwan Ha received the B.S. and M.S. degrees in mechanical engineering from the State University of New York at Binghamton, Binghamton, NY, USA, in 2018 and 2020, respectively, where he is currently pursuing the Ph.D. degree in mechanical engineering with the Opto-Mechanics and Physical Reliability Laboratory.

His current research interests include chip component self-alignment and solder joint fatigue under thermal loading.

Karthik Arun Deo received the B.S. degree in mechanical engineering from the Amrita School of Engineering, Vallikavu, India, in 2015, and the M.S. degree in thermal engineering from IIT Madras, Chennai, India, in 2019. He is currently pursuing the Ph.D. degree in mechanical engineering with the Opto-Mechanics and Physical Reliability Laboratory, State University of New York at Binghamton, Binghamton, NY, USA.

His current research interests include package and board-level reliability and failure analysis.

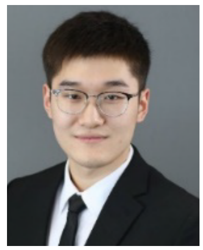

Junbo Yang received the B.S. degree in process equipment and control engineering from the Beijing University of Chemical Technology, Beijing, China, in 2017, and the M.S. degree in mechanical engineering from the State University of New York at Binghamton, Binghamton, NY, USA, in 2019, where he is currently pursuing the Ph.D. degree with the Opto-Mechanics and Physical Reliability Laboratory, Department of Mechanical Engineering.

His current research interests include experiments and simulation to improve the reliability of microelectronics packaging.

Pengcheng Yin (Graduate Student Member, IEEE) received the B.S. degree in mechanical design and manufacture and its automation from the Central South University of Forestry and Technology, Changsha, China, in 2018, and the M.S. degree in mechanical engineering from the State University of New York at Binghamton, Binghamton, NY, USA, in 2020, where he is currently pursuing the Ph.D. degree in mechanical engineering with the Opto-Mechanics and Physical Reliability Laboratory.

He is currently concentrating on designing dynamic impact experiments and shock/impact/vibration simulation of electronic packaging.

Seungbae Park (Senior Member, IEEE) received the Ph.D. degree from Purdue University, West Lafayette, IN, USA, in 1994.

He was a Development and Reliability Engineer with IBM, Armonk, NY, USA, where he was responsible for flip-chip technology. Since 2002, he has been a Professor with the Department of Mechanical Engineering, State University of New York at Binghamton, Binghamton, NY, USA, where he is currently the Director of the Integrated Electronics Engineering Center (IEEC). His current research interests include physical reliability for microelectronics and microelectromechanical systems packaging.

Dr. Park is a fellow of the American Society of Mechanical Engineers (ASME). He has served many technical communities. He was the Chair of the iNEMI's Modeling and Simulation Technical Work Group and the Electronics Packaging Council in the Society of Experimental Mechanics.